ENERGY DISTRIBUTION OF ELECTRONS TO THE CURRENT IN METAL-SEMICONDUCTOR SYSTEM

By M. J. Małachowski

Military Academy of Technology, Warsaw*

(Received July 29, 1972; Revised paper received January 12, 1973)

Energy distributions of electrons emitted from the semiconductor into the metal and in the opposite direction are considered. Numerical computations for metal-*n* type silicon system are carried out. The influence of the donor impurity concentration, applied voltage and temperature on the distribution are examined. Particular attention is given to the case of heavily doped semiconductor. Results of the numerical computations are presented graphically in the form of the dependence of the normalized electron flux emitted from the semiconductor into the metal and *vice versa* as a function of the electron energy.

1. Introduction

Metal-semiconductor (M–S) systems made on lightly doped semiconductors have been extensively studied and thermionic emission has been established as the mechanism of current flow. In this case the potential barrier at the contact interface is so wide that the only way the electrons can reach from the semiconductor into the metal is by emission over the barrier.

The tunneling probability increases with semiconductor doping since the depletion region width decreases, which makes the potential barrier thinner and easer to tunnel through.

The useful characteristic energy E_{00} is defined as [1]

$$E_{00} = \frac{qh}{4\pi}\left(\frac{N}{m^*\varepsilon}\right)^{1/2} = 1.85 \cdot 10^{-11}\left(\frac{N}{m_r\varepsilon_r}\right)^{1/2} eV \tag{1}$$

where q is the electronic charge, h is Planck's constant, N the impurity concentration in units of cm^{-3}, m_r is the tunneling effective mass measured in units of the free electron mass $m_0(m^* = m_r m_0)$ and ε_r is the static dielectric constant measured in units of the free space permittivity $\varepsilon_0(\varepsilon_s = \varepsilon_r \varepsilon_0)$.

* Address: Katedra Fizyki Ogólnej, Wojskowa Akademia Techniczna, 00-908 Warszawa, Poland.

The ratio kT/E_{00} is a measure of the relative importance of the thermionic process in relation to the tunneling process [2, 3].

1. In the low doping range where $kT/E_{00} \gg 1$, thermionic emission (TE) of electrons over the barrier becomes dominant (Fig. 1a).

2. As the semiconductor doping increases (Fig. 1b) the barrier becomes thinner and exited electrons with sufficient thermal energy tunnel through the midsection of the energy

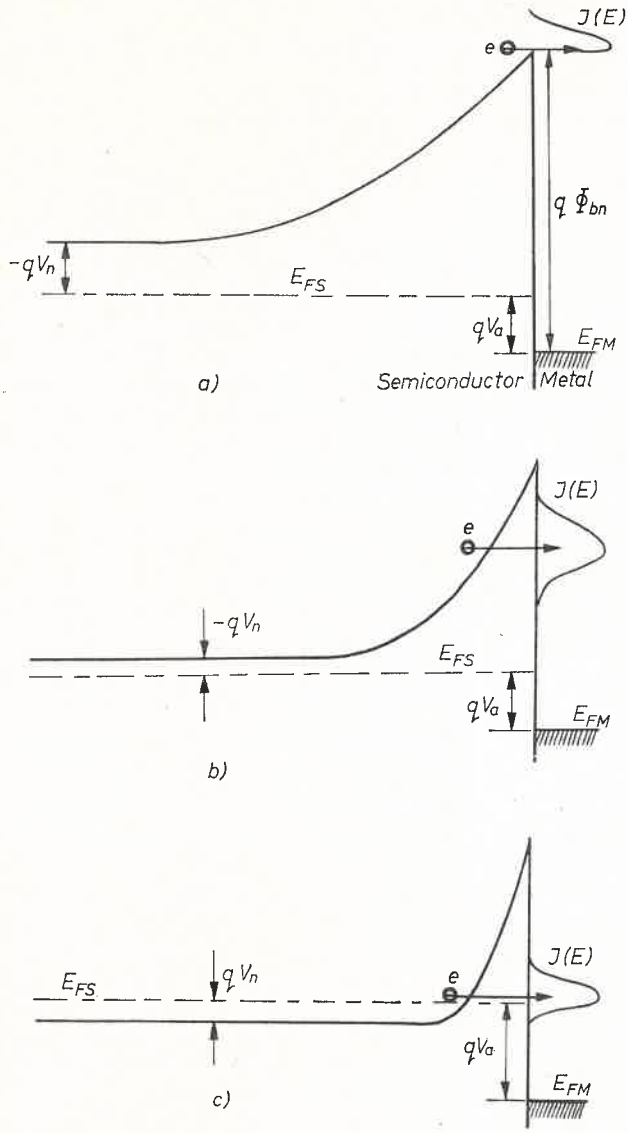

Fig. 1. Energy band diagrams of metal-*n* type semiconductor contacts under forward bias voltage: a) lightly doped semiconductor (TE emission), b) heavily doped semiconductor (TFE emission), c) very heavily doped semiconductor FE emission). $J(E)$ represents the energy distribution of the electrons emitted from the semiconductor into the metal

barrier from the metal to the semiconductor. This current density is referred to as thermionic field emission (TFE). In this case the thermionic and tunneling processes are comparable ($kT/E_{00} \approx 1$).

3. When the semiconductor is very heavily doped, or at very low temperatures ($kT/E_{00} \ll 1$), the current is carried by electrons tunneling from the Fermi level in the semiconductor into the metal (Fig. 1c). This process is called field-emission (FE).

In this paper, the energy distribution of electrons during the current flow in the M–S barrier is considered. The influence of the donor impurity concentration, applied voltage and temperature on the distribution are numerically examined for a metal-n type silicon system. Results of the numerical computations presented graphically concern the TE, TFE and FE cases help in understanding the current flow processes in the M–S system.

In Ref. [12] an analysis of a similar distribution in the metal-insulator-metal system is made.

2. Carrier transport equation

The energy band diagram of a metal-semiconductor barrier under equilibrium conditions is shown in Fig. 2, where Φ_{bn} is the M–S barrier height, V_b is the built-in potential, $\Delta\varphi$ is the barrier lowering due to image force, E_{FM} and E_{Fs} are the Fermi energy

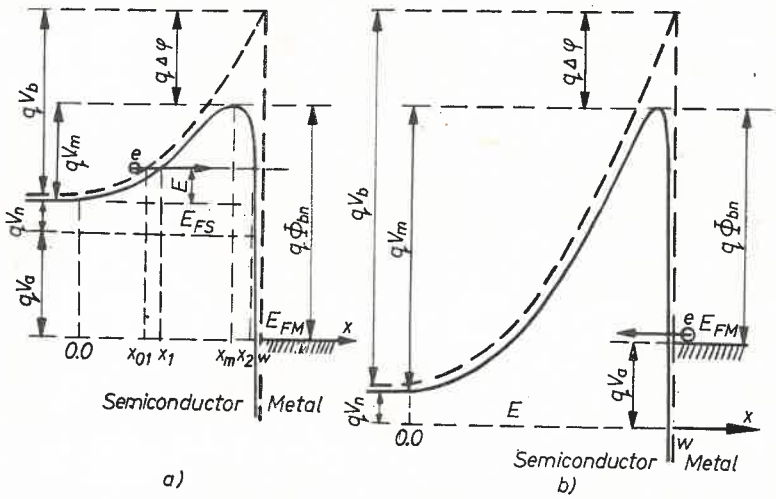

Fig. 2. Band diagrams of metal-n type semiconductor contact under: a) direct bias voltage, b) reverse bias voltage

of the metal and the semiconductor respectively, w is the depletion region with, V_a is the applied voltage. Fig. 2a shows the forward and Fig. 2b the reverse biased M–S barriers.

A general expression for the electron current density J flowing from the semiconductor into the metal or from the metal into the semiconductor is given by

$$J = \int_0^\infty J(E_x)dE_x = \int_0^{qV_m} J_1(E_x)dE_x + \int_{qV_n}^\infty J_2(E_x)dE_x \tag{2}$$

where E_x is a measure of the energy associated with the motion of the electron normal to the S–M interface, qV_m is the barrier maximum level. The energies are measured from the band edge in the semiconductor as shown in Fig. 2. The first term od equation (2) represents the contribution from tunneling (TFE and FE), and the second term is the thermionic component (TE). The products $J_1(E_x)\,dE_x$ or $J_2(E'_x)\,dE_x$ represent the net current density contributed from electrons with energies associated with the motion normal to the junction, placed between E_x and E_x+dE_x or E'_x and $E'_x+dE'_x$, where $E'_x > qV_m$. Functions $J_1(E_x)$ and $J_2(E'_x)$ are given by

$$J_1(E_x)dE_x = P_1(E_x, m^*)N(E_x)dE_x \tag{3a}$$

$$J_2(E'_x)dE_x = P_2(E'_x, m^*)N(E'_x)dE_x \tag{3b}$$

where $N(E_x)dE_x$ represents the net flux density of electrons with energies between E_x and E_x+dE_x, $P_1(E_x, m^*)$ is the transmission coefficient of the barrier, $P_2(E'_x, m^*)$ is the transmission coefficient for the electrons that have energy E'_x greater than the barrier maximum qV_m.

Transmission coefficient for tunnel emission is given by

$$P_1(E_x, m^*) = [1+\exp Q(E_x, m^*)]^{-1} \tag{4}$$

where

$$Q(E_x, m^*) = \frac{2\sqrt{2m^*}}{\hbar}\int_{x_1}^{x_2}\sqrt{qV(x)-E_x}\,dx \tag{5}$$

where $qV(x)$ is a barrier energy profile similar to that shown in Fig. 2 and x_1 and x_2 are, respectively the small and large roots of $qV(x)-E_x=0$. $P_1(E_x, m^*)$ is the transmission coefficient if tunneling occurs in the interval between the classical turning points x_1 and x_2. The transmission coefficient $P_2(E'_x, m^*)$ for thermionic emission is not unity. We can use Kemble's approximation [4].

$$P_2(E'_x, m^*) = 1-P_1(E_x, m^*) \tag{6}$$

where $E'_x = 2qV_m-E_x$, Thus the transmission coefficient at an energy ΔE above the top of the image force lowered barrier equals one minus the transmission coefficient at an energy ΔE below the top of that barrier.

The quantity $N(E_x)$, commonly referred to as supply function, in the case of an electron flowing in the semiconductor-metal direction, is given by [14]:

$$N(E_x) = \frac{A^*T}{k}\left\{\ln\left[1+\exp\left(\frac{E_{FS}-E_x}{kT}\right)\right]-\ln\left[1+\exp\left(\frac{E_{FS}-E_x-qV_a}{kT}\right)\right]\right\} \tag{7}$$

and in the case of the metal-semiconductor direction, given by [13]:

$$N(E_x) = \frac{AT}{k}\left\{\ln\left[1+\exp\left(\frac{E_{FM}-E_x}{kT}\right)\right]-\ln\left[1+\exp\left(\frac{E_{FM}-E_x-qV_a}{kT}\right)\right]\right\}$$

$$\text{for } E_x > E_{FM} \tag{8}$$

and

$$N(E_x) = \frac{AT}{k} \ln\left[1+\exp\left(\frac{E_{FM}-E_x}{kT}\right)\right] \quad \text{for} \quad E_x < E_{FM} \tag{8'}$$

where A and A^* are the Richardson constants for metal and for semiconductor respectively [1]. E_{FS} can be obtained from the relation $V_n = \frac{kT}{q} \ln \frac{N_c}{N}$, where qV_n is the energy difference between the conduction band edge and the Fermi level in the bulk of the semiconductor, N_c is the conduction band effective density of states. At high concentrations, the Fermi energy position can be obtained more exactly for example from the paper [9].

In the present work the quantities $J_1(E_x)$ and $J_2(E_x')$ (Eqs (3a) and (3b)) will be separately calculated for various doping concentrations, applied voltages and temperatures as a function of energies E_x. In the calculation of J_1 and J_2, the main difficulties lie in evaluation of the transmission coefficient P_1.

3. Barrier height in the M–S system

The barrier heights in the M–S system are, in general, determined by both the metal work function and the surface states. When a metal makes intimate contact with a semiconductor, the Fermi levels in the two materials must be coincident, so the Fermi level in the semiconductor is lowered by an amount equal to the difference between the two work functions. This potential difference $q\Phi_m - q(\varphi_s - V_n)$ is called the contact potential, where $q\Phi_s$ is the electron affinity. The barrier height $q\Phi_{bn}$ which must surmount electrons travelling from metal to semiconductor (neglecting the Schottky lowering $q\Delta\varphi$), is given by

$$q\Phi_{bn} = q(\Phi_m - \varphi_s). \tag{9}$$

The Schottky lowering as a result of the image force and the electric field is given by [4, 5]:

$$\Delta\varphi = \frac{1}{2^{3/4}\sqrt{\pi}} \left(\frac{q}{\varepsilon_s}\right)^{3/4} (NV_b)^{1/4} = 5.22 \cdot 10^{-7} \frac{(V_b N)^{1/4}}{\varepsilon_r^{3/4}} \text{ [Volts]} \tag{10}$$

where V_b is the barrier height that must surmount electrons trawelling from semiconductor to metal if the Schottky lowering is neglected.

We consider a semiconductor with acceptor surface states whose density is very large. As a result, the barrier height is determined by the property of the semiconductor surface, is independent of the metal work function and is given by

$$q\Phi_{bn} = E_g - q\varphi_0 \tag{11}$$

where E_g is the band gap and φ_0 is the energy difference between the Fermi level and the valence-band edge at the surface before the M–S contact is formed. This specifies the level below which all surface states must be filled for charge neutrality at the surface [6].

Equations (9) and (11) are the two limiting cases obtained from a more complicated equation given by Sze (7). This equation can be approximately reduced to the following form:

$$\Phi_{bn} = c_1\Phi_m + c_2 \tag{12}$$

c_1 and c_2 can be determined experimentally: *i. e.* for *n*-type Si $c_1 = 0.27 \pm 0.05$ and $c_2 = -(0.55 \pm 0.22)$V, for CdS $c_1 = 0.38 \pm 0.16$ and $c_2 = -(1.2 \pm 0.77)$ V.

The barrier height which must surmount electrons travelling from semiconductor to metal, lowered by the Schottky effect, is given by:

$$V_m = V_b - \Delta\varphi \tag{13}$$

where

$$V_b = \Phi_{bn} - V_a - V_n \tag{14}$$

$V_b < \Phi_{bn}$ if the metal is positive, and for sufficiently high opposite polarization , $V_b > \Phi_{bn}$.

4. Barrier shape in the M–S system

1. Schottky lowering neglected. Fig. 2 shows the potential barrier shape in the M–S system. It can be shown [8] that solving of the Poisson's equation for this problem gives a barrier shape of the following form

$$V = V_b y^2 \tag{15}$$

or

$$v(y) = y^2 \tag{15'}$$

where $y = x/w$ is the normalized distance, x being the distance from the point in the bulk semiconductor where depletion region ends (Figure 2),

$$w = \sqrt{\frac{2\varepsilon_s V_b}{qN}} \tag{16}$$

is the barrier region width, and $v(y) = V/V_b$ is the normalized potential in the barrier region.

2. The Schottky lowering included. The lowering of the metal work function by an amount $\Delta\varphi$ as a result of the image force and the electric field, is called the Schottky effect. This effect changes the parabolic one-dimentional potential distribution defined by equation (15) to the following equation [4]:

$$V = V_b y^2 - \frac{q}{16\pi\varepsilon_s(w-x)}$$

which, in normalized form, becomes

$$v(y) = y^2 - \frac{v_0}{1-y} \tag{17}$$

where

$$v_0 = \frac{1}{16\pi}\sqrt{\frac{N}{2}}\left(\frac{q}{\varepsilon_s V_b}\right)^{3/2} = 3.44\cdot 10^{-14}\,\frac{\sqrt{N}}{(\varepsilon_r V_b)^{3/2}}. \tag{18}$$

In equation (17) not only the doping concentration but also the applied voltage are included because V_b depends on V_a (Eq. 14).

5. Evaluation of classical turning points

The values of classical turning points x_1 and x_2, *i. e.* the intersection points of the barrier with the tunneling level E_x, were needed in the computation of the transmission coefficient $P_1(E_x)$ (Eq. 4).

1. Schottky lowering neglected. In this case, the normalized intersection points can be obtained from (15′). The normalized tunneling level is $E_x/V_b \equiv v$. Two intersection points can be obtained from the equation $v(y) = y^2$, *i. e.* $y_{01} = \sqrt{v}$ and $y_{02} = 1$.

2. Schottky lowering included. Equation (17) is a cubic equation in y. The appropriate solution for normalized intersection points is given by:

$$y_1 = \frac{1}{3} + \frac{2a}{3}\sqrt{1+3v}\cos\left(60^0 + \frac{\varphi}{3}\right)$$

$$y_2 = \frac{1}{3} + \frac{2}{3}\sqrt{1+3v}\cos\left(b60^0 - \frac{\varphi}{3}\right) \tag{19}$$

where φ is the smallest positive angle which satisfies the equation

$$\cos\varphi = \frac{9v-1+13.5v_0}{(1+3v)^{3/2}},$$

$a = 1$, $b = 1$ if $\cos\varphi > 0$, and $a = -1$, $b = 0$ if $\cos\varphi < 0$.

3. Schottky lowering included — approximate expressions. If in Eq. (17) we put $v_0/(1-y) = v_0/(1-\sqrt{v})$ and $v(y) = v$ one of the intersection points becomes

$$y_1 = \sqrt{v + \frac{v_0}{1-\sqrt{v}}} \tag{20}$$

and if we put $y^2 = 1$ we obtain the second intersection point:

$$y_2 = 1 - \frac{v_0}{1-v}. \tag{21}$$

Formulation (20) and (21) does not apply in the top barrier region. To find the position y_m of the barrier maximum, $d[v(y)]/dy$ of equation (17) is equated to zero. The root of the

cubic equation nearest to and less than unity gives

$$y_m = \frac{2}{3}\left[\cos\left(60^0 + \frac{\alpha}{3}\right) + 1\right] \quad \text{where} \quad \cos\alpha = 1 - 6.75 v_0.$$

The approximate solution of the cubic equation has the following form:

$$y_m = 1 - \sqrt{\frac{v_0}{2}}. \tag{22}$$

From (22) and (17) we obtain the normalized maximum barrier height

$$v_m = 1 - 2^{3/2}\sqrt{v_0} + \frac{v_0}{2} \tag{23}$$

and the barrier lowering:

$$\frac{\Delta\varphi}{q} \equiv (1 - v_m)V_b = 2^{3/2}\sqrt{v_0}\, V_b - \frac{1}{2} v_0 V_b. \tag{24}$$

It can be shown from (24) and (18) that the first term of the right-hand-side of equation (24) coincides with expression (10). The second term of equation (24) my be neglected in the case of low concentrations, but not for heavy concentrations.

6. The transmission coefficient

Normalization of $qV(x)$, E_x and x in equation (4) gives:

$$P_1(v) = \left[1 + \exp\left(\frac{8\pi V_b m^* \varepsilon_s}{hN} \int_{y_1}^{y_2} \sqrt{v(y) - v}\, dy\right)\right]^{-1}. \tag{25}$$

The integral $I = \int_{y_1}^{y_2} \sqrt{v(y) - v}\, dy$ can be evaluated through numerical analysis by substituting appropriate quantities from equations (19) and (17). It is difficult to express I in closed forms. We shall, however, find approximate analytic expressions for I. If the Schottky effect is included the integrating area can be divided into two parts: (y_1, y_3) and (y_3, y_2) (Fig. 3). Then the integration concerns the dashed part of the parabolic barrier which is very close to the real barrier. It is clear that

$$I \approx \int_{y1}^{y_3} \sqrt{v(y) - v}\, dy + (v_m - v)(y_2 - y_3).$$

Substituting in I the approximate expressions $v(y) = y^2$, $y_1 = \sqrt{v}$, $y_2 = 1 - \dfrac{v_0}{1 - v,}$ $y_3 = \sqrt{v_m}$ and integrating

$$P_1(v) \approx [1 + e^{Q(v)}]^{-1} \tag{26}$$

where

$$Q(v) = \frac{8\pi V_b}{h}\sqrt{\frac{m^*\varepsilon_s}{N}}\left[\sqrt{v_m - v}\left(1 - \frac{v_0}{1-v} - \frac{\sqrt{v_m}}{2}\right) - \frac{v}{2}\ln\frac{\sqrt{v_m}+\sqrt{v_m - v}}{\sqrt{v}}\right].$$

If $v = 0$

$$P_1(0) = \exp\left[-\frac{8\pi V_b}{h}\sqrt{\frac{m^*\varepsilon_s v_m}{N}}\left(1 - v_0 - \frac{v_m}{2}\right)\right]$$

and if $v \to v_m$, $P_1(v) \to 0.5$.

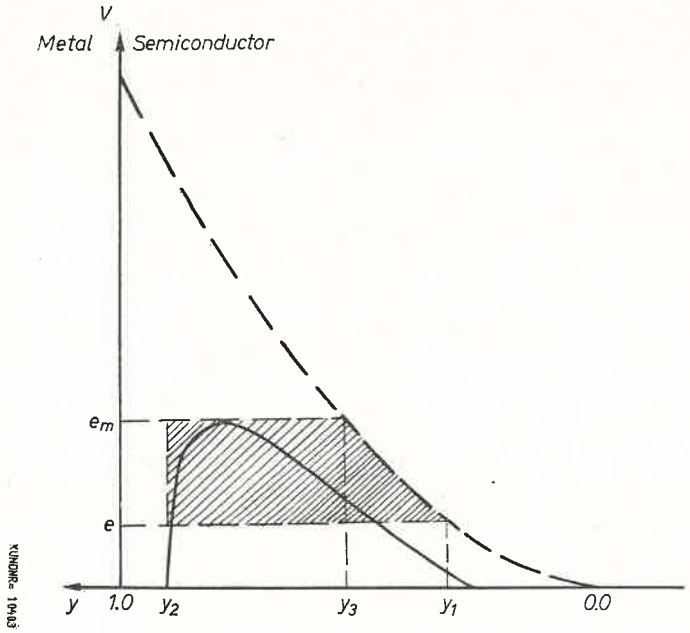

Fig. 3. Potential barrier shape in metal-*n* type semiconductor contact

7. Energy distribution of electrons contributing to the current in the M–S system

The energy distribution of electrons which contribute to the current can be obtained from the calculation of the "tunnel current" function $J_1(E_x)$ (Eq. (3a)) and of the "thermionic current" function $J_2(E_x)$ (Eq. (3b)). The "tunnel current" and "thermionic current" functions can be found by substituting $N(E_x)$ form (7), $P_1(E_x)$ from (26) and $P_2(E_x')$ from (6). Equations (3a) and (3b) can be used for various M–S systems. To obtain a physical picture for the energy distribution of the electrons flowing in the M–S interface an *n*-type silicon-metal structure was chosen.

To calculate the energy distribution (3a) and (3b) we use the pertinent Richardson constant [10] A^*, and dynamic dielectric constant [7]. In silicon the tuneling effective mass is a function of temperature and of doping concentration. For dopings lower than 5.10^{17} cm^{-3}, the mass m^* is essentially the same as that of 5.10^{17} cm^{-3}. For higher dopings, however, m^* increases with the doping. To calculate the energy distribution we use the

tunneling effective mass from [11], and assume that the barrier height of the Si-metal system equals 0.8 eV (for Si–Au diodes).

The results of calculation of the energy distribution of electrons which contribute to the current in the M–Si system polarized in the forward and reverse directions are presented graphically. This distribution is showed schematically in Fig. 1 as $J(E)$. In Figs 4a, b, c the doping concentration, applied voltage and temperature are used as parameters. Five doping concentrations (10^{16}, 10^{17}, 10^{18}, 10^{19}, 10^{20} cm^{-3}) were considered at various temperatures and applied voltage conditions. The vertical lines between leters M and S represent a one-dimensional M–S barrier lowered by the Schottky effect (from 0.5 to 0.8 eV above the metal Fermi level). The curves at the left- hand-side of the barrier represent the energy distributions of electrons flowing in the forward direction, and those to the right — in the reverse direction. In Figs 4a, b, c, the Fermi levels

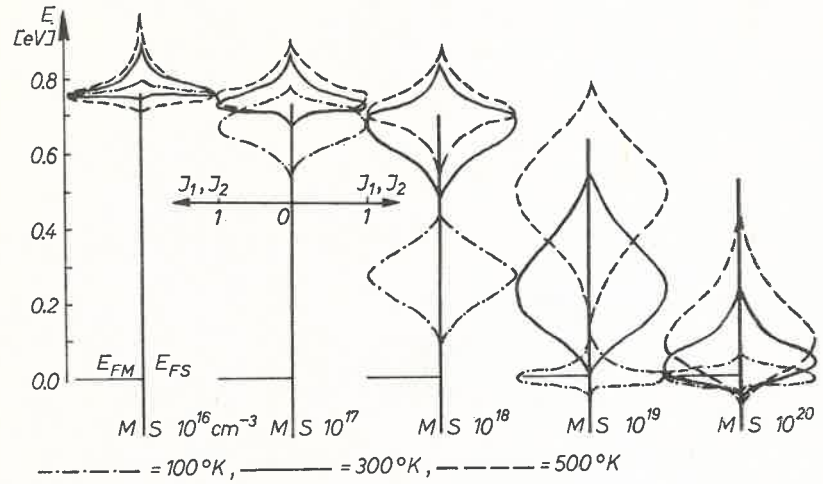

a

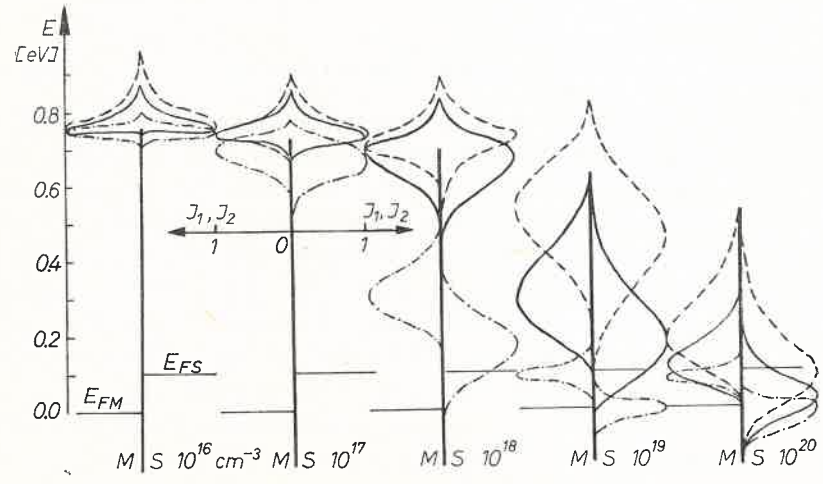

b

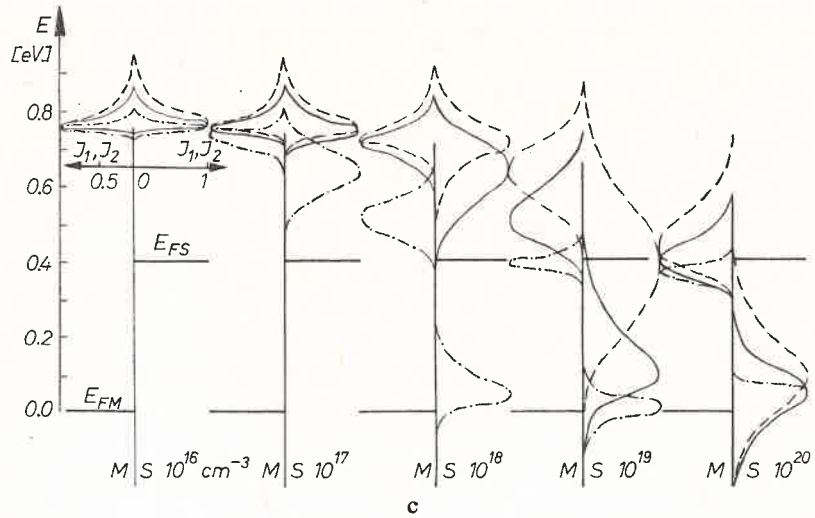

c

Fig. 4. Energy distribution of the electrons emitted from the metal into the semiconductor and *viceversa* as a function of the concentration, temperature and applied voltage. Vertical lines are one dimensional barriers. Right and left-hand-side normalized distribution curves concern reverse and direct polarized M-Si system respectively. a) $V_a = \pm 10^{-3}$ V, b) $V_a = \pm 0.1$ V, c) $V_a = \pm 0.4$ V

in the metal and in the semiconductor are marked for the case when the M–S system is polarized in the forward direction (E_{Fs} is higher than E_{FM} by qV_a). The Fermi level of a semiconductor polarized in the reverse direction is not shown in Figs 4a, b, c. E_{Fs} in this case is lower than E_{FM} by qV_a (Fig. 2b).

The results of the energy distribution calculations presented in Figs 4a, b, c concern the tunneling range. The distribution in this case becomes a strong function of doping, temperature and applied voltage. This distribution is peaked at a certain energy E_m. In the thermionic emission range E_m coincides with qV_m both in the forward and reverse directions. In the tunneling range E_m becomes a strong function of doping, temperature and applied voltage.

From Eqs (3a) and (3b) the rectification ratio can be evaluated by computing the quantity

$$n = \left.\frac{J_1(E_x)}{J_2(E'_x)}\right|_{E_x = E_m} \tag{27}$$

Of course n is not a well known rectification ratio of the M–S system, because neither $J_1(E_x)$ nor $J_2(E'_x)$ represent the current flowing in this system.

8. *Summary*

Examination of Figs 4a, b, c and the values of n (Eq. 27) reveals the following features of the energy distribution of electrons emitted from the semiconductor into the metal and from the metal into the semiconductor:

1. Ionized impurity concentration. As concentration increases, the depletion width decreases, which in turn causes the transmission coefficient for tunneling to increase.

If the barrier is thin enough, tunnelling dominates the carrier transport process, as can be seen in Figs 4a, b, c. The energy level E_m at which the energy distribution function is peaked decreases as the concentration increases until it reaches the semiconductor Fermi level in the direct-polarized M–S barrier and the metal Fermi level in the reverse-polarized barrier.

The current densities of both polarization directions becomes comparable with each other in the high concentration region, even at fairly high voltages.

The distribution curve is broader in the TFE region that in TE or FE regions.

2. Applied voltage. As the voltage applied to the M–S system increases, the barrier width and height become smaller, which in turn causes both the direct and the reverse current density to increase. The current densities of both polarization directions become comparable with each ather at a voltage which is very low in the low concentration region and at higher voltages as the concentration increases. As the applied voltage increases the distribution curve in the direct polarization case becomes thinner and in the reverse polarization case-broader.

3. Temperature. For higher temperatures more carriers are excited above the Fermi level. Both the direct and the reverse current density increase. As the temperature decreases the distribution curves at high and low concentration regions ($\leqslant 10^{16}$ cm^{-3} and $\geqslant 10^{19}$ cm^{-3}) become narrower. The current which flows through the barrier becomes more monoenergetic. The energy level E_m becomes lower as the temperature decreases. For 100°K $E_m < qV_m$ already at about 10^{17} cm^{-3}, and reaches the Fermi level of the metal at about 10^{19} cm^{-3}. It can be seen from Figs 4a, b, c that for temperatures above 100°K and concentrations below 10^{17} cm^{-3} the TE process is a dominant one. For doping concentrations above 10^{17} cm^{-3} the TEF process becomes dominant. The FE process dominates for low temperatures and high concentrations only.

The results of the calculation of the energy distribution of the electrons which contribute to the current in the M–S system presented in Figs 4a, b, c cover the practical ranges of doping, applied voltage and temperature. These results are believed to be useful in reaching a better understanding of electrical processes in M–S interfaces of many semiconductors devices.

REFERENCES

[1] F. A. Padovani, R. Stratton, *Solid State Electronics*, **9**, 695 (1966).
[2] C. R. Crowell, V. L. Rideout, *Solid State Electronics*, **12**, 89 (1969).
[3] A. Y. C. Yu, *Solid State Electronics*, **13**, 239 (1970).
[4] V. L. Rideout, C. R. Crowell, *Solid State Electronics*, **13**, 993 (1970).
[5] C. Y. Chang, S. M. Sze, *Solid State Electronics*, **13**, 727 (1970).
[6] J. Bardeen, *Phys. Rev.*, **71**, 717 (1947).
[7] S. M. Sze, *Physics of Semiconductor Devices*, John Willey and Sons, New York 1969.
[8] M. J. Małachowski, *Biuletyn WAT*, **20**, 43 (1971).
[9] D. Dale Kleppinger, F. A. Lindholm, *Solid State Electronics*, **14**, 407 (1971).
[10] C. R. Crowell, *Solid State Electronics*, **8**, 395 (1965); **12**, 55 (1969).
[11] C. Y. Chang, Y. K. Fang, S. M. Sze, *Solid State Electronics*, **14**, 541 (1971).
[12] M. J. Małachowski, *Acta Phys. Polon.*, **33**, 693 (1968).
[13] W. Tantraporn, *IEEE Trans. Electron Devices*, USA, **ED-19**, No 3, 331 (1972).
[14] S. J. Fonash, *Solid State Electronics*, **15**, 783 (1972).